Polyelectrolyte effects in model photoresist developer solutions

Vivek M. Prabhu,[a] Ronald L. Jones, Eric K. Lin, and Wen-li Wu
Polymers Division, National Institute of Standards and Technology, Gaithersburg, Maryland 20899-8541

(Received 2 January 2003; accepted 19 May 2003; published 3 July 2003)

We demonstrate that the deprotected photoresist poly(4-hydroxy styrene) is a polyelectrolyte when dissolved in aqueous base solutions. This polyelectrolyte effect manifests itself by the well-known monomer–monomer correlations as measured by small-angle neutron scattering. The correlation peak at the finite wave vector is a function of the solution ionic strength and polymer concentration. The weakening of the polyelectrolyte effects with added salts and excess base is also demonstrated. These studies emphasize the role of salt additives and aqueous base concentration and their influence on equilibrium solution properties such as the second virial coefficient and single chain radius of gyration. The fundamental role of these equilibrium properties with respect to the dissolution process is discussed. [DOI: 10.1116/1.1591742]

I. INTRODUCTION

The chemical amplification process has been the subject of intense industrial research for over 20 years[1] and has recently been applied in semiconductor manufacturing. During this time the simple idea of using the difference in miscibility between radiation exposed and masked regions has been utilized in different chemical forms, namely positive-tone and negative-tone resists. While the idea has remained constant, many problems such as transparency, contamination, substrate compatibility, and performance remain to be addressed for each upcoming technological node. One apparent constant in the positive-tone resist technology is the utilization of an aqueous base developer.

For the APEX-E photoresist the poly(4-*t*-butoxycarbonyloxystyrene) (PBOCSt) is deprotected to the form of poly(4-hydroxystyrene) (PHOSt) after photoacid generation from ultraviolet (UV) light exposure during the postexposure bake (PEB) step. The PHOSt-rich regions are subsequently dissolved leaving the nanoscopic features of the UV-exposed regions with an industry standard 0.26 N tetramethyl ammonium hydroxide (TMAH) solution. The ability to dissolve selectively the PHOSt-rich domains is accomplished because TMAH is regarded as a better solvent for the PHOSt than the PBOCSt.

Recent models describe photoresist dissolution as a series of chemical reaction-rate equilibrium steps, whereby the depletion of the soluble element follows a rate equation. This species is subject to a solubility criterion as in the critical ionization model.[2] This approach has related dissolution rate and surface roughness from theory to experiment. Another approach that also models dissolution as a sequence of chemical reaction-rate equilibrium steps is that by Hunek and Cussler.[3] In this method, the boundary conditions are related to the phase diagram and diffusivity can be modeled explicitly into the mass transfer coefficients. Having set up the rate equations, the rate-limiting step is chosen appropriately to simplify the theory and compare with experimental data. One promising aspect in both models is the potential of using equilibrium constants for predicting experimental dissolution behavior. We anticipate that for future photoresist formulations an independent measurement will be required to select the correct physics, such as ionization or gelation, to provide the input into the model. The above-cited models and references therein provide a successful framework for which the details of the resist–developer interactions can be incorporated.

The purpose of this article is to highlight the importance of polyelectrolyte effects for the understanding of deprotected model photoresist polymers in aqueous base solutions. It is well known that for the case of PHOSt in an aqueous base the high *p*H of the solution renders the phenol-like monomers to be soluble. From elementary organic chemistry tables, the pKa of a phenol proton[4] is 10. Thus, for *p*H greater than 10 the equilibrium favors the deprotonated state. The *p*H of a 0.26 N TMAH solution is 13.31, which strongly favors the conjugate base form. *This chemical equilibrium state is the origin of the intended miscibility*. This is a fact as the bare PHOSt is not miscible in pure water. The idea of applying chemical equilibria to low molar mass molecules is well established and works well. However, when the charged monomer is now connected to its neighbors to make a polymer, the influence of correlations between monomers is important.[5] Simple acid-base equilibrium, based upon well-defined chemical equations, neglect all these correlations.

These monomer density–density correlations are measured in a small-angle neutron scattering (SANS) experiment and provide insight into the essential physics that will help understand the roles of dissolution inhibitors in photoresist formulations and dissolution additives in aqueous base developers. The manner in which the correlations are measured will be discussed, as well as the important physical parameters controlling them. This article is intended to highlight how the ionized form of model photoresist solutions behave differently with respect to their organic solvent counterparts.

We have examined the small-angle neutron scattering by deuterated model photoresist polymers in a typical casting

[a]Author to whom correspondence should be addressed; electronic mail: vprabhu@nist.gov

solvent propylene glycol methyl ether acetate (PGMEA) and several aqueous base developer solutions sodium hydroxide (NaOH), potassium hydroxide (KOH), and tetramethyl ammonium hydroxide (TMAH), with and without added salts. The detailed experiment is in Sec. II, followed by scattering preliminaries in Sec. III. In Sec. IV we present our main results and their discussions before concluding in Sec. V.

II. EXPERIMENT

The deuterated poly(4-hydroxystyrene) (d_3-PHOSt) was custom synthesized by Polymer Source, Inc., Dorval, Quebec,[6] with weight-average relative molecular weight of $M_{r,n}=8750\ \mathrm{g\,mol^{-1}}$ and polydispersity $M_{r,w}/M_{r,n}=1.07$. This solid glassy powder was dissolved directly in aqueous base solutions with and without added salts. Tetramethyl ammonium hydroxide solutions were prepared by dilution of a stock solution (mass fraction of 10%), purchased from Aldrich Chemicals, using deionized water with resistivity 18.0 $\mathrm{M\Omega\,cm}$ purified by a Milli-Q UF Plus system. Sodium hydroxide (NaOH) and potassium hydroxide solutions were prepared by quantitative addition of analytical grade salt pellets to a known volume of deionized water to achieve the desired normality of 0.26 N. To prepare solutions with added salts, potassium chloride (KCl), and sodium chloride (NaCl) were dissolved directly in the corresponding aqueous base solutions: NaCl in NaOH and TMAH solutions and KCl in KOH solutions.

It should be noted here that to prepare a $0.0388\ \mathrm{g\,cm^{-3}}$ solution of d_3-PHOSt in 0.26 N TMAH we first prepared a $0.0821\ \mathrm{g\,cm^{-3}}$ solution in 0.55 N TMAH, followed by dilution with deionized water. We did this because the direct preparation of the solution was not feasible. The polymer never became soluble in the transparent form, it was always cloudy with sedimenting particles. Leaving the solution with constant stirring and heat to 50 °C did not improve the solubility, nor did two months of storage. However, the high 0.55 N TMAH solution readily dissolved, even at $0.0821\ \mathrm{g\,cm^{-3}}$, and upon dilution remained clear with a slightly golden color, as is common with all the PHOSt solutions. This methodology of dilution was observed to be unnecessary with the same KOH or NaOH solutions. This problem, whether kinetic or thermodynamic, was repeatedly observed and its physical basis is of uncertain origin and must influence the dissolution process. Barring a kinetically hindered dissolution process, we can conclude that TMAH is fundamentally different in its association with the PHOSt monomers, as compared to NaOH and KOH at low pH and/or the degree of ionization required for miscibility is quantitatively different for dissolution. These effects may be supported by the observations reported by Honda *et al.*[7,8] with the formation of a stable complex, except that in our equilibrium solutions the result may be more appropriately termed a stable–miscible complex. According to Honda *et al.* the complex formation is displaced upon addition of NaOH, which appears consistent with our observations of PHOSt solubility in NaOH. However, even with the presence of a stable–miscible complex, the polyelectrolyte behavior persists, as observed by SANS.

Small-angle neutron scattering was performed on the NG1 guide 8 m instrument at the National Center for Neutron Research (NCNR), National Institute of Standards Technology. A seven-position sample changer was used to examine the small-angle scattering by dilute polymer and pure solvent solutions in which the scattering contrast was achieved by using partially deuterated poly(4-hydroxystyrene) (d_3-PHOSt) in light water (H_2O) containing various levels of basic and salt components. The raw neutron scattering count rate, normalized by the incident flux, was measured directly with a two-dimensional area detector using a 1.27 cm sample aperture and 4.7 cm beam stop. The wavelength of the neutrons used was 6.0 Å with a spread ($\Delta\lambda/\lambda$) of 0.12. Two configurations were used with a fixed sample–detector distance of 3.8 m by changing the detector tilt angle that leads to scattering wave vector (q) ranges of 0.01–0.1 and 0.01–0.15 $\mathrm{Å^{-1}}$, for tilt angles of 1.5° and 3.5°, respectively. The raw two-dimensional scattered intensity was corrected for sample transmission, detector efficiency, cadmium blocked-beam background, and scattering by an empty quartz cell on a detector cell-by-cell basis. This was followed by circularly averaging the two-dimensional corrected scattered intensity and by using a light water secondary standard the data were placed on an absolute (±5%) differential scattering cross-section scale.[9] The sample cells were stainless steel with 1 mm path length. The cells had two detachable quartz windows that are screw sealed with O rings. The uncertainties are calculated as the estimated standard deviation of the mean. In the case where the limits are smaller than the plotted symbols, the limits are left out for clarity. Fits of the scattering data are made by a weighted least-squares minimization and the error corresponds to one standard deviation to the fit.

III. SCATTERING PRELIMINARIES

A. Dilute neutral polymer solutions

We have examined the scattering by deuterated model photoresist polymers in a typical casting solvent propylene glycol methyl ether acetate and several aqueous base developer solutions: sodium hydroxide, potassium hydroxide, and tetramethyl ammonium hydroxide, with and without added salts. The coherent neutron scattering is feasible due to the scattering length density difference between the deuterium-labeled d_3-PHOSt monomers (b_m/ν_m) and the proton-rich solvent (b_s/ν_s). The SANS experiments performed here measures the monomer density–density correlations arising from both inter and intra-chain denoted by the total scattering structure factor $S_T(q)$. Here we present the scattering equation in which C_m is the monomer concentration and N the degree of polymerization:

$$I(q)=\left(\frac{b_m}{\nu_m}-\frac{b_s}{\nu_s}\right)^2 C_m N S_T(q). \tag{1}$$

TABLE I. Experimental quantities.

	d_3-PHOSt	PGMEA	H_20
$M_{r,w}$ (g mol^{-1})	8750	⋯	⋯
PDI ($M_{r,w}/M_{r,n}$)	1.07	⋯	⋯
M_i (g mol^{-1})	123.0 (monomer)	132.16	18.0
v_i (cm^3 mol^{-1})	84.0	136.53	18.063
b_i (cm)	60.281×10^{-13}	12.42×10^{-13}	-1.675×10^{-13}

In the limit of dilute solutions, a Zimm plot may be performed, which shows the dependence of the scattered intensity as a function of polymer concentration by plotting $HC_m/I(q)$ vs $k'C_m+q^2$. H is a neutron optical constant $[b_v^2N_a(\nu_m/M_m)^2]$ where b_v^2 is the scattering length density difference between monomer repeat unit and solvent, N_a Avogadros number, ν_m and M_m are the molar volume and molecular mass of a monomer, respectively, all provided in Table I; k' is an arbitrary scaling factor that is independent of the extrapolated quantities.[10,11] From a double extrapolation in concentration and scattering wave vector, the *z*-average radius of gyration (R_g), second virial coefficient (A_2) and weight-averaged relative molar mass ($M_{r,w}$) are obtained.

This Zimm methodology applies for systems dominated by short-ranged interactions, as in neutral polymer solutions. However, for the case of strong correlations, as in aggregating colloid systems or electrolytic systems in which the interactions are long-ranged, the classical Zimm plot may lead to ambiguous results.[12] This is because the static structure becomes concentration dependent, rather than having a randomized system as in dilute polymer solutions.

B. Polyelectrolyte scattering preliminaries

When a macromolecule contains charged monomers or charged segments the scattering behavior becomes very different, in particular at low solution ionic strength. This is true for polyelectrolyte gels,[13,14] charged colloidal particles,[15] charged dendrimers,[16] semiflexible polyelectrolytes,[17–19] and even linear flexible polyelectrolytes.[15,20] This class of systems remains to be understood at the level of their neutral counter parts. This article does not intend to, nor comes close to, summarizing this field as it pertains to the problem of photoresist solutions. However, one is referred to one of several review articles.[12,15,20,21]

One main feature regarding the small-angle scattering by a low-ionic strength semidilute polyelectrolyte solution is the appearance of a broad scattering peak at a position of $q_m \neq 0$. This is in direct contrast to that observed in neutral linear polymer mixtures, in which the maximum in the scattered intensity is observed only at $q=0$. One theoretical achievement in gaining a better understanding of low-ionic strength polyelectrolyte solutions is from a model calculation for the scattering using a random phase approximation (RPA) that predicts this high-q scattering trend exhibited by polyelectrolytes.[21–24] This theory uses the main result from the Debye–Hückel theory to model the interaction potential between two charged statistical segments. The predicted scattering peak position dependence on polymer concentration, salt concentration, and temperature qualitatively agree with experiment. However, the RPA prediction fails to recover the correct scaling laws for the peak maximum. Its use to understand quantitative information such as the Flory–Huggins interaction parameter has limited success due to several deficiencies (a) anomalous scattering observed in the low-q limit, (b) poor understanding of ionic strength contributions from polymer counterions versus added salt ions, (c) effect of density and chain fluctuations, and (d) incomplete consideration of the true multicomponent nature of the solution. In any event, the RPA calculation does highlight two important trends observed that will be demonstrated in this article, namely, the dependence of peak position on polymer concentration and ionic strength and thus presents itself as a very simple theory to gain insight.

The dependence of the peak position (q_m) is the following:

$$q_m \cong \left[\left(\frac{6w_c\phi N}{R_g^2}\right)^{1/2} - \kappa^2\right]^{1/2}, \tag{2}$$

where κ^2 is the inverse-square Debye length, proportional to the solution ionic strength, w_c represents the strength of the screened Coulombic interaction and is a function of the degree of ionization of the polymer, ϕ is the polymer volume fraction, and N the degree of polymerization. The inverse-square Debye length is given by the following formula:

$$\kappa^2 = 4\pi l_B N_A\left(\sum_\gamma Z_\gamma^2 C_\gamma\right), \tag{3}$$

where the sum over all added electrolyte species γ includes added salts as well as basic ions, and l_B is the Bjerrum length, which is 7 Å at 25 °C in water. The value of κ^{-1} represents the Debye screening length, the range over which electrostatics are important. For instance a 0.26 N solution of either TMAH, KOH, or NaOH will have κ^{-1} of 6.0 Å, assuming each has the same activity at the equivalent prepared concentrations; this length decreases further to 2.9 Å at 1.1 N. The addition of salt to these basic solutions decreases the Debye screening length even further. In principle, once the Debye length is reduced to the length scale of the persistence length, then the system is fully screened. One will also notice that the valence of the ion is squared, leading to the fact that multivalence salts can be more effective at lower concentrations in screening.

According to Eq. (2) increased ionic strength leads to a shift in the peak wave vector to lower q values. Similarly, with increased polymer concentration the peak shifts to higher values. These trends are both observed experimentally. The theoretical origin of this peak according to the RPA can be explained as follows: the presence of the bare repulsive screened Coulombic potential with strength w_c leads to a repulsion between monomers and is wave vector dependent. This repulsion between monomers suppresses long-length scale fluctuations, thus leading to the lowered scattered intensity in the low-q limit. This wave vector dependent interaction is now coupled to the usual monomer–

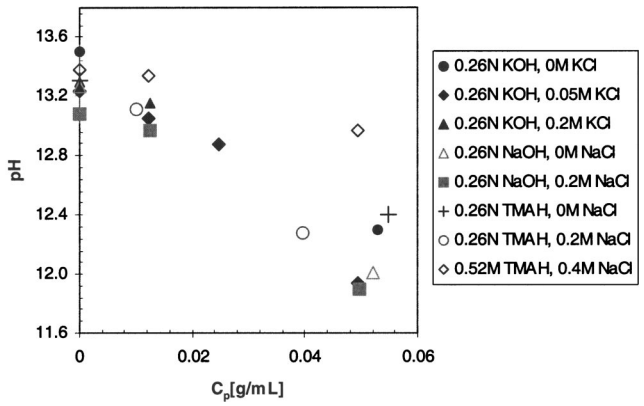

FIG. 1. *p*H dependence on polymer concentration measured for several aqueous base and added salt concentrations indicated in the legend. The experimental standard uncertainty in the measured *p*H is ± 0.01 units, less than the size of the symbols used.

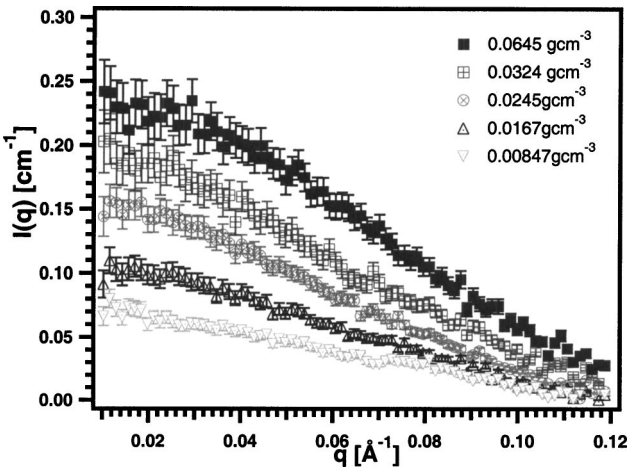

FIG. 2. Small-angle neutron scattering by *d*-PHOSt in PGMEA. Concentrations are provided in the legend. The scattering behavior is typical of neutral polymer solutions. The uncertainties shown are calculated as the estimated standard deviation of the mean.

monomer correlations, exemplified by the Debye structure factor, which has enhanced fluctuations in the low-q region due to chain statistics, along with a limiting decay of $1/q^2$ in the high-q limit. The competition between the suppression of fluctuations in the low-q region by electrostatics and decay in fluctuations according to chain statistics leads to the peak in the total scattering structure factor and is tuned by varying the aforementioned variables. By increasing the ionic strength, the compressibility at larger length scales increases leading to an increase in the observed intensity at low-q region. By increasing the polymer concentration, the typical correlation length decreases, thus leading to the shift of the peak position to higher q at fixed ionic strength, similar in effect to that of neutral polymer solutions. The basis for using the RPA theory is to understand salient features of polyelectrolyte scattering. In the following sections, we will identify a few qualitative polyelectrolyte behaviors present in the photoresist solutions.

IV. RESULTS AND DISCUSSIONS

A. Concentration dependence of *p*H

We have measured the *p*H, when possible, for solutions of pure aqueous base and the change upon addition of PHOSt, as shown in Fig. 1. We have found that the *p*H is systematically lowered upon adding PHOSt, which is consistent with the titration of the hydroxyl proton. This is observed for the three bases studied and also with and without added salts. Thus, in the following discussions regarding the phase behavior of these solutions, the *p*H is a function of polymer concentration. The contribution of free ions from the base developer to the screening is also variable and in principle must be known before calculating the Debye screening length. While this complicates any analysis, it illustrates that a depletion of base at an interface may develop during the dissolution process and far from the interface we expect strong screening due to the presence of base. At this interface the polymer concentration will be high and require an equivalent amount of base to titrate each available hydroxyl proton.

B. Scattering by d_3-PHOSt in PGMEA

Due to the low molecular mass of the d_3-PHOSt and its contrast with the solvent, neutron scattering provides a reasonable q-range and resolution for such small structures. In our case the d_3-PHOSt is only deuterated along the main chain. A significant improvement in scattering contrast could be achieved with higher levels of deuteration, even for dilute solutions, above the relatively high scattering solvent. The scattering by dilute solutions of d_3-PHOSt in PGMEA (0.00847, 0.0167, 0.0245, 0.0324, and 0.0645) $\mathrm{g\,cm^{-3}}$ reveals scattering behavior typical of a neutral polymer in an organic solvent. As shown in Fig. 2, the scattered intensity decays monotonically with increasing wave vector and the absolute intensity, which is proportional to concentration, decreases with decreasing concentration. The results of the Zimm plot shown in Fig. 3 lead to a z-averaged radius of gyration of (30 ± 1) Å, a weight-average relative molar mass of (9600 ± 250) $\mathrm{g\,mol^{-1}}$ and second virial coefficient of 1.29×10^{-3} $\mathrm{cm^3\,mol^{-2}\,g^{-2}}$. The fact that the second virial coefficient is positive indicates that PGMEA is a good solvent for PHOSt. We may convert A_2 into the more familiar Flory–Huggins interaction parameter χ, where $\chi = 1/2 - A_2\rho_2^2 v_1$, ρ_2 is the polymer density and v_1 is the partial molar volume of the solvent.[25] This interpretation leads to a χ of 0.122 at 25 °C. Knowledge of the fundamental interaction parameters can help understand the effects of swelling at interfaces and the dissolution process, since the swelling is a result of the osmotic driving force of solvent into the glassy polymer.

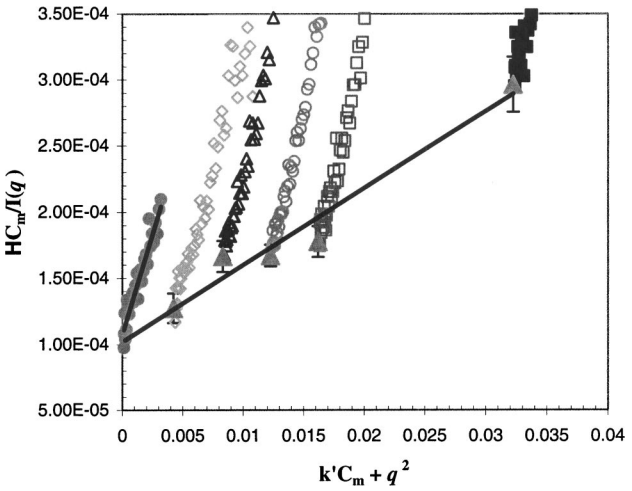

FIG. 3. Zimm plot analysis for the scattering by d-PHOSt in PGMEA. The results are a radius of gyration of 30 ± 1 Å, weight-average relative molar mass of $9600\pm250\ \mathrm{g\,mol^{-1}}$ and second virial coefficient of $1.29\times10^{-3}\ \mathrm{cm^3\,mol^{-2}\,g^{-2}}$. Fits to the data are shown as solid lines which were obtained by a weighted least-squares minimization and the uncertainty is one standard deviation to the fit.

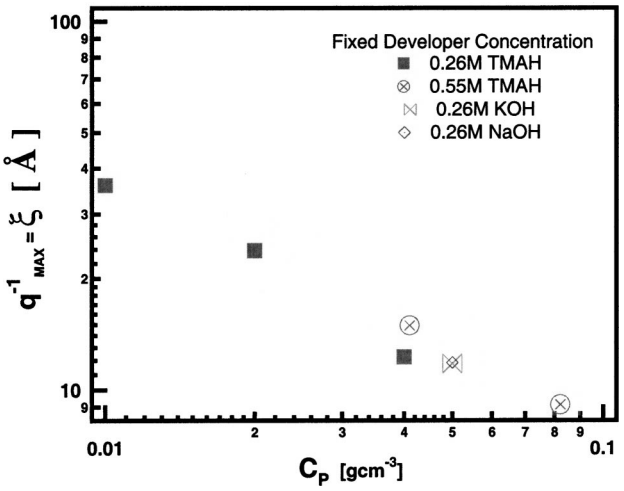

FIG. 5. Variation of inverse polyelectrolyte peak with d_3-PHOSt concentration for several different aqueous base solutions given in the legend. The experimental standard uncertainty is smaller than the symbols and left out for clarity. The main text references the data with the relative uncertainty.

C. Scattering by d_3-PHOSt in aqueous base with and without added salt

The PHOSt in casting solvent represents the essential physics of a system with short-ranged interactions in dilute solutions. The experimental observations for the PHOSt in aqueous developer solutions are significantly different. We show the scattering behavior difference for $0.0374\ \mathrm{g\,cm^{-3}}$ d_3-PHOSt dissolved in PGMEA and $0.0388\ \mathrm{g\,cm^{-3}}$ d_3-PHOSt dissolved in 0.26 N TMAH in Fig. 4. The d_3-PHOSt in PGMEA behaves as a typical neutral polymer solution as described earlier, while a broad peak is observed for the d_3-PHOSt in 0.26 N TMAH. This scattering peak is similar to that observed in semidilute polyelectrolyte solutions.[26–28] It suggests that long-ranged electrostatic interactions are present, leading to a suppression of fluctuations in the low-q region that gives rise to the broad peak. Even though the mass concentrations are equal, the presence of the peak indicates a strong interaction between polyelectrolyte segments in solution. This strong repulsive interaction leads to a chain expansion beyond its Gaussian theta-coil dimension and has been the subject of numerous investigations.[29–31] What is not observed, due to the low q resolution, is that the intensity increases strongly for q less than $0.01\ \mathrm{Å^{-1}}$. This low-q upturn is ubiquitous in low-ionic strength polyelectrolyte solutions and is attributed to an aggregation or multi-chain clustering in solution. The influence of this unresolved problem on photoresists is tempting to infer.

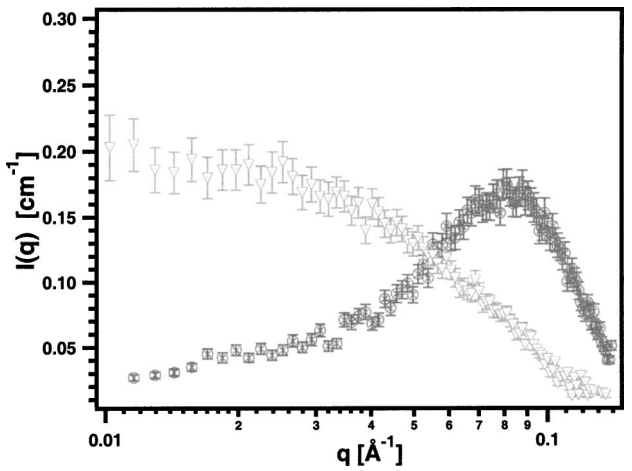

FIG. 4. Small-angle neutron scattering by $0.0374\ \mathrm{g\,cm^{-3}}$ d-PHOSt in PGMEA and $0.0388\ \mathrm{g\,cm^{-3}}$ d-PHOSt in 0.26 N TMAH, the ∇ and $\otimes$ symbols, respectively. The uncertainties shown are calculated as the estimated standard deviation of the mean.

These observations suggest that in the presence of the aqueous base solution, that is un-buffered, the chemical equilibrium between a protonated and deprotonated state favors the deprotonated hydroxyl form of PHOSt, which can now be considered a polyelectrolyte. This titration of the PHOSt monomers results in an ionic character from which the bare interaction between charged monomers is Coulombic in nature. This leads to a monomer–monomer repulsion that is now coupled to the monomer connectivity resulting in the scattering peak at $q\neq0$ as described previously. The remaining basic components can be considered to contribute to the total solution ionic strength and the range of the electrostatic interaction calculated from the Debye screening length. We present the inverse scattering peak position as a function of polymer concentration in Fig. 5. Typically, for low-ionic strength semidilute polyelectrolyte solutions, the inverse peak position scales with polymer concentration as $q^{-1}\sim C_p^{-1/2}$. From a fit to the entire data set we find the exponent of the concentration to be -0.68 ± 0.03, rather than -0.5, which is anticipated due to the fact that these solutions are not under the class of ''salt-free'' polyelectrolyte solutions. Any added electrolytes, due to the un-buffered solu-

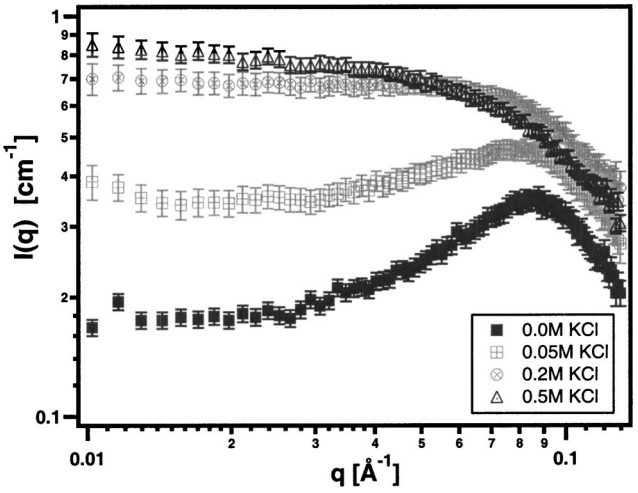

FIG. 6. Small-angle neutron scattering by a 0.053 g cm^{-3} *d*-PHOSt in 0.26 N KOH with varying added KCl salt from (0 to 0.5) M, as indicated in the legend, solvent scattering is subtracted. The broadening and elimination of the polyelectrolyte peak is observed, consistent with the screening of the electrostatic interaction. The uncertainties shown are calculated as the estimated standard deviation of the mean.

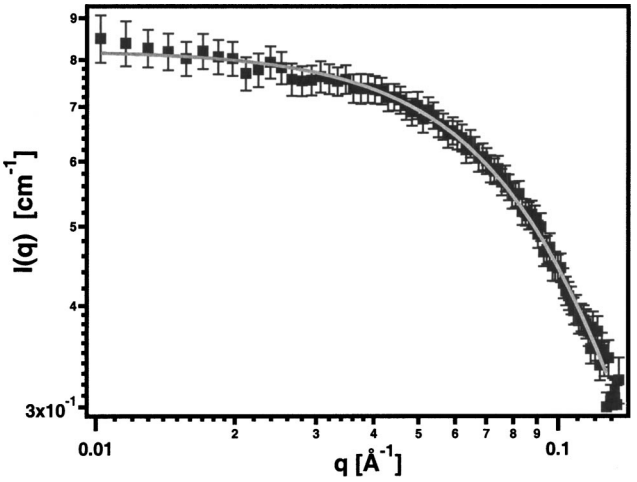

FIG. 7. High salt SANS scattering from 0.053 g cm^{-3} *d*-PHOSt in 0.26 N KOH with 0.5 M KCl. The scattered intensity could be adequately fit, solid line, with the Debye structure factor, providing an apparent radius of gyration of (14.0±1.0) Å. The uncertainties shown are calculated as the estimated standard deviation of the mean.

tions, will lead to screening which tends to change the scaling behavior. In addition, the system is not in the semidilute solution region, as the estimated overlap concentration for an extended chain is 0.03 g cm^{-3}, while that for the corresponding theta-coil dimensions is 0.084 g cm^{-3}.

Again, it can be shown that the polyelectrolyte effects can be tuned by several measures, such as by changing the solution dielectric constant,[32] adding salt,[21,33] or copolymer content.[34] In this case we examine, in particular, the influence of added salt. The scattering behavior of 0.053 g cm^{-3} d_3-PHOSt in 0.26N KOH with varying added KCl salt from (0 to 0.5)M is shown in Fig. 6.

In principle, if the electrostatic interaction becomes screened then the collective and configurational properties of a polyelectrolyte solution should resemble that of a neutral polymer solution.[35,36] This was observed in the limit of high salt for intrinsically flexible polyelectrolytes as shown previously by SANS.[34,37] For the no added salt condition with *d*-PHOSt concentration fixed at 0.053 g cm^{-3} in 0.26N KOH, we observe the scattering peak position, q_m, to be $q_m = (0.0849 \pm 0.0003)$ Å^{-1}. Maintaining the *d*-PHOSt concentration fixed, an increase in salt concentration to 0.05 M decreases q_m to (0.0781 ± 0.0003) Å^{-1}, consistent with the trends predicted from the RPA theory. For the higher salt concentrations 0.20 and 0.5 M a peak is no longer resolved and the scattering form at high salt is similar to that of the neutral polymer solution, which is consistent with a screening of the electrostatic interactions. We did attempt to perform a Zimm plot in this case, but, the statistics were so poor that we could not place confidence in the final extrapolated quantities. However, we can provide an estimate for the radius of gyration, R_g, by directly fitting the measured scattered intensity with the Debye structure factor, as shown in Fig. 7, leading to an apparent R_g of (14.0±1.0) Å, which is significantly smaller than the R_g obtained in PGMEA, which was (30.0±1.0) Å. This does suggest that upon addition of excess salt the solvent quality is sufficiently poor to lead to chain collapse.

The scattering behavior of PHOSt in aqueous developer is a general phenomenon and is not dependent on the type of base. For instance, we examined PHOSt in three different aqueous buffers, NaOH, TMAH, and KOH, as shown in Fig. 8. All of these samples show the same essential feature, namely a correlation peak, which is a function of polymer concentration and added salt.

D. PHOSt in 1.1 N TMAH aqueous base

We also examined the scattering behavior of PHOSt in the presence of excess base, 1.1 N TMAH. Under this condition

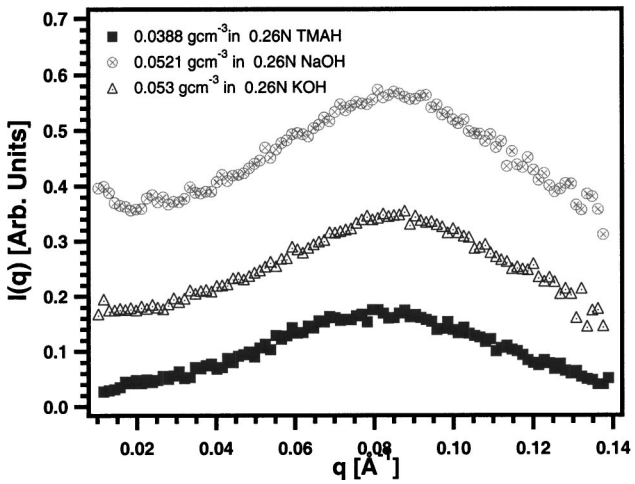

FIG. 8. Polyelectrolyte peak for three different aqueous base buffer solutions 0.26 N TMAH, 0.26 N KOH, and 0.26 N NaOH, with (0.0388, 0.0521, and 0.053) g cm^{-3} d_3-PHOSt concentration, respectively. The uncertainties are calculated as the estimated standard deviation of the mean, in this case the limits are smaller than the plotted symbols and are left out for clarity.

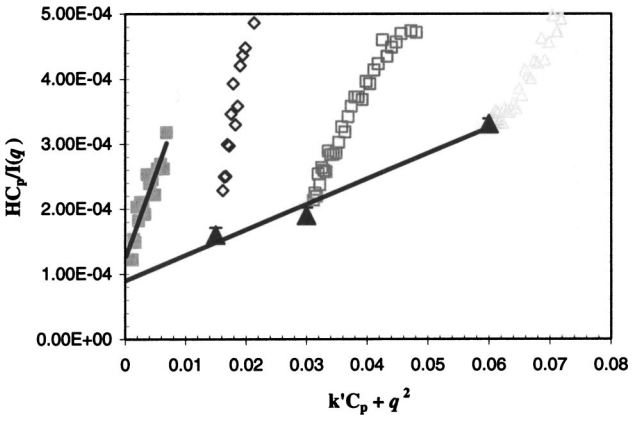

FIG. 9. Zimm plot for 1.1 N TMAH with *d*-PHOSt. The results are a radius of gyration of (29 ± 3) Å, a weight-average relative molecular weight of 9600 $g\,mol^{-1}$ and a second virial coefficient (A_2) of 2.7×10^{-3} $cm^3\,mol^2\,g^{-2}$. Fits of the data are shown in the solid lines are obtained from a weighted least-squares minimization and the error is one standard deviation to the fit.

all electrostatic interactions should be screened due to the high concentration of basic components, similar to the influence of added salt, leading to a vanishing Debye screening length. We were able to obtain a Zimm plot as shown in Fig. 9 and recovered the molecular weight of 9600 $g\,mol^{-1}$ and a radius of gyration of (29 ± 3) Å (see, also, Table II). The second virial coefficient A_2 is 2.7×10^{-3} $cm^3\,mol^2\,g^{-2}$. The chain dimension is slightly larger than that of bulk polystyrene in the melt which is 23.5 Å, for an equivalent degree of polymerization. However, experiments for PHOSt in the melt in which the excluded volume would be screened, are necessary for a quantitative comparison, since the poly(4-hydroxystyrene) persistence length may differ from polystyrene. There appears to be an excluded volume present as measured from the positive second virial coefficient. We obtain an effective χ of 0.40 at 25 °C. This estimate for χ can be used to predict the phase behavior of this system. However, it is likely that this value of χ would be ionic strength dependent. Future experiments such as a series of light scattering experiments at high ionic strengths and varied temperature would explore new areas in the phase behavior and phase separation of model photoresist systems. The influence of copolymer composition tunes the charge density of the chain and is an important parameter to investigate, since a critical fraction or range of copolymer composition is required to observe miscibility.

TABLE II. Zimm plot results.

	PGMEA	1.1N TMAH
$M_{r,w}$ ($g\,mol^{-1}$)	9600 ± 250	9648 ± 2000
$\langle R_g^2\rangle_Z^{1/2}$ (Å)	30 ± 1	29 ± 3
A_2 ($cm^3\,mol^2\,g^{-2}$)	1.29×10^{-3}	2.7×10^{-3}
χ (25 °C)	0.122	0.40

V. CONCLUDING REMARKS

Early experiments on dilute solutions of polyelectrolytes with added salts demonstrate that the second virial coefficient, determined by static light scattering, is a strong function of the ionic strength.[38,39] In these studies it was observed that the second virial coefficient decreases with increasing salt concentration. Thus, the solvent quality is lowered with the addition of salt, by reducing the tendency for repulsion between chains. In the limit of excess salt, barring precipitation of the polymer, the electrostatic influence will be screened. We have presented the case of the second virial coefficient at both high salt and high base concentrations eliminating the polyelectrolyte correlations. While we were not able to demonstrate the experiments as functions of salt concentration, this work can easily be extended to the case that uses the more conventional static light scattering with higher molecular weights and much more dilute solutions. The behavior is universal with regards to the effect of added salt. Thus, we now understand an important contribution to the driving force for dissolution, solvent quality, is a function of any added electrolytes as well as the final *p*H of the solution.

Recent experiments demonstrate a salt-concentration dependent dissolution rate. However, at salt concentrations approaching molar, the dissolution rate depends in a nonlinear fashion on the concentration of added salts,[40] from which nonlinear activity coefficients and miscibility of salts can inherently complicate the physics. In the critical ionization model of Willson *et al.*[40] the result of Bahe is used to model the activity coefficient.[41,42] Our results demonstrate that in order to fully screen the electrostatics and eliminate the correlation peak, the salt concentration is between 0.2 and 0.5 M corresponding to a bare Debye length between 6.8 and 4.2 Å. Now, if the solvent quality tends to become poorer in the limit of very high salt concentrations, then one contribution to the overall dissolution rate decrease with excess salt could be the lower solvent quality. Of course, the diffusion coefficient is a strong function of ionic strength. At the lowest added salt concentrations an increase in the dissolution rate is captured with the nonlinear activity coefficient, but may also be related to an increased osmotic driving force for mixing ions at the dissolution front, while maintaining good polymer solvent quality. At higher ionic strengths, the poorer solvent quality dominates leading to a peak in the dissolution rate dependence. The observation that the dissolution rate peak position is independent of the 1:1 electrolyte suggests that such a simple crossover to poor solvent behavior must be independent of the solvent quality between the polymer and electrolyte solution. If each salt had a specific effect with the polymer, then the dependence on solvent quality would lead to a variation in the observed dissolution rate peak position.

This article highlights the manner in which all future developer–photoresist solutions will behave in the limit of low ionic strength. Their behavior is that of a polyelectrolyte which should have consequences during the time-dependent dissolution process. At the interface of the dissolution front

the monomers that come into the range of the titrating basic ions will tend to shift their equilibrium to that of the charged state. Once this occurs, the configurational properties change dramatically leading to chain expansion. The consequences of this on the stability of the dissolving interface are unknown. Depending on the depth at which the solvent and any added ions can penetrate the dissolution front, the collective behavior of charged polymers must differ from that of the neutral polymer counterparts, which has been well studied to date. Thus, in the spirit of this work, many experiments are necessary to understand the inter-phase properties during the kinetics of dissolution. Since this dissolution front is revealed to be a steady-state front, after an initial induction period, experiments with nanometer resolution are necessary to explore this poorly understood problem of dissolution. In particular, at the penetration front, since the local concentration of polyelectrolyte is high and represents either a semidilute or concentrated solution, experiments in this regime would highlight any new physics of dense polyelectrolyte solutions. The collective diffusion of charged polymers, and hence, all transport related properties, are strongly dependent on controllable experimental variables such as ionic strength, solvent mixtures, molecular weight, chain branching, temperature, salt mixtures, and valence. Thus, knowledge of the controlling parameters in polyelectrolytes will help to expand the understanding of next-generation developer solutions and/or resist formulations.

ACKNOWLEDGMENTS

This work was supported by the Defense Advanced Research Projects Agency under Grant No. N66001-00-C-8083 and the NIST Office of Microelectronics Programs. Two of the authors (V.M.P. and R.L.J.) are grateful for support from the National Research Council–National Institute of Standards and Technology Postdoctoral Fellowship Program.

[1]H. Ito, IBM J. Res. Dev. **44**, 119 (2000).
[2]F. A. Houle, W. D. Hinsberg, and M. I. Sanchez, Macromolecules **35**, 8591 (2002), and references therein.
[3]B. Hunek and E. L. Cussler, AIChE J. **48**, 661 (2002).
[4]S. N. Ege, *Organic Chemistry, Structure, and Reactivity* (Heath, Lexington, MA, 1994).
[5]L. W. Flanagan, C. L. McAdams, W. D. Hinsberg, I. C. Sanchez, and C. G. Willson, Macromolecules **32**, 5337 (1999).
[6]Certain commercial equipment and materials are identified in this article in order to specify adequately the experimental procedure. In no case does such identification imply recommendation by the National Institute of Standards and Technology, nor does it imply that the material or equipment identified is necessarily the best available for this purpose.
[7]K. Honda, B. T. Beauchemin, R. J. Hurditch, and A. J. Blakeney, Proc. SPIE **1672**, 297 (1992).
[8]R. R. Dammel, *Diazonaphthoquinone-Based Resists* (SPIE, Bellingham, WA, 1993), p. 114.
[9]G. D. Wignall and F. S. Bates, J. Appl. Crystallogr. **20**, 28 (1987).
[10]J. des Cloizeaux and G. Jannink, *Polymers in Solution, Their Modeling and Structure* (Oxford University Press, New York, 1990).
[11]J. S. Higgins and R. S. Stein, J. Appl. Crystallogr. **11**, 346 (1978).
[12]H. Dautzenberg, *Polyelectrolytes: Formation, Characterization, and Application* (Hanser, New York, 1994).
[13]M. Shibayama and T. Tanaka, J. Chem. Phys. **102**, 9392 (1995).
[14]M. Shibayama, F. Ikkai, Y. Shiwa, and Y. Rabin, J. Chem. Phys. **107**, 5227 (1997).
[15]H. Matsuoka and N. Ise, Adv. Polym. Sci. **114**, 187 (1994).
[16]G. Nisato, R. Ivkov, and E. J. Amis, Macromolecules **32**, 5895 (1999).
[17]M. Milas, M. Rinaudo, R. Duplessix, R. Borsali, and P. Lindner, Macromolecules **28**, 3119 (1995).
[18]B. Guilleaume, J. Blaul, M. Wittemann, M. Rehahn, and M. Ballauff, J. Phys.: Condens. Matter **12**, A245 (2000).
[19]R. Borsali, H. Nguyen, and R. Pecora, Macromolecules **31**, 1548 (1998).
[20]S. Forster and M. Schmidt, Adv. Polym. Sci. **120**, 51 (1995).
[21]J.-L. Barrat and J.-F. Joanny, Adv. Chem. Phys. **XCIV**, 1 (1996).
[22]T. A. Vilgis and R. Borsali, Phys. Rev. A **43**, 6857 (1991).
[23]V. Y. Borue and I. A. Erukhimovich, Macromolecules **21**, 3240 (1988).
[24]M. J. Grimson, M. Benmouna, and H. Benoit, J. Chem. Soc., Faraday Trans. 1 **84**, 1563 (1988).
[25]*Polymer Handbook*, edited by J. Brandrup and E. H. Immergut (Wiley, New York, 1989).
[26]N. Ise, T. Okubo, S. Kunugi, H. Matsuoka, K. Yamamoto, and Y. Ishii, J. Chem. Phys. **81**, 3294 (1984).
[27]M. Nierlich, C. E. Williams, F. Boue, J. P. Cotton, M. Daoud, B. Farnoux, G. Jannink, C. Picot, M. Moan, C. Wolff, M. Rinaudo, and P. G. de Gennes, J. Phys. (France) **40**, 701 (1979).
[28]K. Kaji, H. Urakawa, T. Kanaya, and R. Kitamaru, J. Phys. (France) **49**, 993 (1988).
[29]F. Boue, J. P. Cotton, A. Lapp, and G. Jannink, J. Chem. Phys. **101**, 2562 (1994).
[30]M. N. Spiteri, J. P. Cotton, A. Lapp, and G. Jannink, Phys. Rev. Lett. **77**, 5218 (1996).
[31]V. M. Prabhu, M. Muthukumar, Y. B. Melnichenko, and G. D. Wignall, Polymer **42**, 8935 (2001).
[32]A. Sehgal and T. Seery, Macromolecules **31**, 7340 (1998).
[33]Y. Ikeda, M. Schmidt, M. Beer, and K. Huber, Macromolecules **31**, 728 (1998).
[34]W. Essafi, F. Lafuma, and C. E. Williams, *Structure of Polyelectrolyte Solutions at Intermediate Charge Densities* (American Chemical Society, Washington, DC, 1994).
[35]M. Muthukumar, J. Chem. Phys. **105**, 5183 (1996).
[36]M. Muthukumar, J. Chem. Phys. **107**, 2619 (1997).
[37]B. D. Ermi and E. J. Amis, Macromolecules **30**, 6937 (1997).
[38]T. Nicolai and M. Mandel, Macromolecules **22**, 438 (1989).
[39]A. Takahashi, T. Kato, and M. Nagasawa, J. Phys. Chem. **71**, 880 (1967).
[40]P. C. Tsiartas, L. W. Flanagin, W. D. Hinsberg, C. L. Henderson, I. C. Sanchez, R. T. Bonnecaze, and C. G. Willson, Macromolecules **30**, 4656 (1997).
[41]L. W. Bahe, J. Phys. Chem. **76**, 1062 (1972).
[42]L. W. Bahe and D. Parker, J. Am. Chem. Soc. **97**, 5664 (1975).